Stability Analysis and Design of Composite Structures

Mark D. Denavit, A.M.ASCE[1]; Jerome F. Hajjar, F.ASCE[2]; Tiziano Perea, A.M.ASCE[3]; and Roberto T. Leon, Dist.M.ASCE[4]

Abstract: The direct analysis method is the primary means of assessing system stability within a standard specification. This method, and in particular its use of reduced stiffness, has been thoroughly validated for use in frames consisting of structural steel members. However, appropriate stiffness reductions have not yet been established nor has the method as a whole been validated for frames with steel-concrete composite columns. Through comparisons between second-order inelastic analysis results and results from the design methodology on a parametric suite of small frames, the current design provisions are evaluated in this paper. The results indicate that while the current design provisions are safe and accurate for the majority of common cases, there exist cases in which the current provisions result in high levels of unconservative error. Modifications to the current design provisions are proposed to address these issues. **DOI: 10.1061/(ASCE)ST.1943-541X.0001434.**

Author keywords: Steel-concrete composite; Beam columns; Structural stability; Design; Metal and composite structures.

Introduction

The direct analysis method as defined in the American Institute of Steel Construction (AISC) "Specification for Structural Steel Buildings" (AISC 2010b) provides an accurate and straightforward way of addressing in-plane frame stability in the design process. In this method, required strengths are determined from a second-order elastic analysis in which members are modeled with a reduced rigidity and initial imperfections are either directly modeled or represented with notional lateral loads. Available strengths are then computed based on the unsupported length of the member, eliminating the need to compute an effective length factor.

The validity of the direct analysis approach has been established through comparisons between second-order elastic analyses and second-order inelastic analyses that had been deemed sufficiently accurate to provide a basis for design provisions (Surovek-Maleck and White 2004a, b; Deierlein 2003; Martinez-Garcia 2002). Similar methodologies were utilized to establish the validity of the effective length method (Kanchanalai 1977) as well as the elastic second-order approach within the American Concrete Institute (ACI) code (ACI 2011; Hage and MacGregor 1974).

However, to date no appropriate reduced elastic rigidity values have been developed nor has the direct analysis methodology in general been thoroughly validated for steel-concrete composite columns. To address this current design need, a large parametric study investigating the stability behavior of small, nonredundant frames focusing on the development and validation of direct analysis recommendations for composite systems was conducted and is presented in this paper.

[1]Design Engineer, Stanley D. Lindsey and Associates, Ltd., 2300 Windy Ridge Pkwy SE, Suite 675S, Atlanta, GA 30339 (corresponding author). E-mail: mdenavit@sdlal.com

[2]CDM Smith Professor and Chair, Dept. of Civil and Environmental Engineering, Northeastern Univ., Boston, MA 02115. E-mail: jf.hajjar@neu.edu

[3]Professor, Departamento de Materiales, Universidad Autónoma Metropolitana, Mexico City 02200, Mexico. E-mail: tperea@azc.uam.mx

[4]D.H. Burrows Professor, Via Dept. of Civil and Environmental Engineering, Virginia Tech, Blacksburg, VA 24061. E-mail: rleon@vt.edu

Note. This manuscript was submitted on January 21, 2015; approved on September 4, 2015; published online on October 30, 2015. Discussion period open until March 30, 2016; separate discussions must be submitted for individual papers. This paper is part of the ***Journal of Structural Engineering***, © ASCE, ISSN 0733-9445.

Benchmark Frames

This paper includes a parametric study in which results from second-order inelastic analyses of benchmark composite structures are compared with results from current and proposed design methodologies based on second-order elastic analysis. The results of both are dependent on specific cross section properties and frame configuration. Thus, to ensure broad applicability of the findings, a wide variety of material and geometric properties are examined. Prior benchmark studies to calibrate stability procedures for structural steel systems made use of a set of small nonredundant frames constructed with a $W200 \times 46.1 (W8 \times 31)$ section in either strong or weak axis bending (Kanchanalai 1977; Surovek-Maleck and White 2004b). This set of frames is expanded and generalized for this paper and a variety of composite cross sections are selected (each cross section is used within each benchmark frame to provide a comprehensive set of results). The composite frames and cross sections used in this paper were also used to evaluate and compare current design methodologies according to the AISC specification (2010b) and ACI code (2011) in prior research (Denavit et al. 2014).

Cross Sections

The cross sections chosen for investigation in this paper are categorized into four groups: (1) circular concrete-filled steel tubes (CCFTs), (2) rectangular concrete-filled steel tubes (RCFTs), (3) steel reinforced concrete (SRC) subjected to strong axis bending, and (4) SRC subjected to weak axis bending. Within these groups, sections were selected to span practical ranges of concrete strength, steel ratio ($\rho_s = A_s/A_g$, where A_s is the area of the steel section and A_g is the gross area of the composite section), and reinforcing ratio ($\rho_{sr} = A_{sr}/A_g$, where A_{sr} is the area of reinforcing bars) for the SRC sections (CFTs with longitudinal reinforcing bars are excluded in this paper). Other section properties (e.g., steel yield strength) were taken as typical values. Steel yield strengths were selected as $F_y = 345$ MPa (50 ksi) for wide-flange shapes,

Table 1. Selected Steel Shapes and Reinforcing Configurations (Adapted from Denavit et al. 2014, © ASCE)

Section type	Index	Steel shape or reinforcing configuration	ρ_s or ρ_{sr} (%)
CCFT	A	HSS177.8 × 12.7(HSS7.000 × 0.500)	24.8
	B	HSS254 × 12.7(HSS10.000 × 0.500)	17.7
	C	HSS323.9 × 9.5(HSS12.750 × 0.375)	10.6
	D	HSS406.40 × 6.4(HSS16.000 × 0.250)	5.7
	E	HSS609.6 × 3.2(HSS24.000 × 0.125)[a]	1.9
RCFT	A	HSS152.4 × 152.4 × 12.7(HSS6 × 6 × 1/2)	27.6
	B	HSS228.6 × 228.6 × 12.7(HSS9 × 9 × 1/2)	19.1
	C	HSS203.2 × 203.2 × 6.4(HSS8 × 8 × 1/4)	11.1
	D	HSS228.6 × 228.6 × 3.2(HSS9 × 9 × 1/8)	5.0
	E	HSS355.6 × 355.6 × 3.2(HSS14 × 14 × 1/8)[a]	3.3
SRC (shape)	A	$W360 \times 463$($W14 \times 311$)	11.7
	B	$W360 \times 347$($W14 \times 233$)	8.7
	C	$W360 \times 179$($W12 \times 120$)	4.5
	D	$W200 \times 46.1$($W8 \times 31$)	1.2
SRC (reinforcing)	A	20 #36 (#11)	4.0
	B	12 #32 (#10)	1.9
	C	4 #25 (#8)	0.4

[a]Not a standard section.

$F_y = 290$ MPa (42 ksi) for round hollow structural section (HSS) shapes, $F_y = 317$ MPa (46 ksi) for rectangular HSS shapes, and $F_{ysr} = 414$ MPa (60 ksi) for reinforcing bars. The AISC specification (2010b) prescribes a lower limit of 21 MPa (3 ksi) and an upper limit of 70 MPa (10 ksi) on the concrete strength. Three concrete strengths were selected: $f'_c = 27.6$, 55.2, and 110.3 MPa (4, 8, and 16 ksi). The highest concrete strength exceeds the AISC limit but was included to broaden the comparison and to ensure applicability of the results should the limit be altered in the future.

There is no prescribed upper limit of steel ratio for composite sections within the AISC specification (2010b); however, practical considerations and the dimensions of commonly produced steel shapes impose an upper limit of approximately 25% for CFT and 12% for SRC, although higher ratios can be obtained with built-up sections. The AISC specification (2010b) sets a lower limit of steel ratio for composite sections of 1%. However, a stricter limit is imposed by the maximum permitted width-to-thickness ratios for CFT members. For the steel yield strengths listed previously, the width-to-thickness limits correspond to steel ratio limits of 1.86% for CCFT and 3.16% for RCFT. For SRC members, the AISC specification (2010b) prescribes a minimum reinforcing ratio of 0.4% and no maximum.

Noting these limitations, five round HSS shapes were selected for the CCFT sections, five rectangular HSS shapes were selected for the RCFT sections, and for the SRC sections with outside dimensions of 711 × 711 mm (28 × 28 in.), four wide-flange shapes and three reinforcing configurations were selected (Table 1). For the HSS shapes, the design thickness, equal to 0.93 times the nominal thickness, was used for all calculations. The reinforcing steel was assumed to have a cover from the edge of the concrete to the edge of the bar of 48 mm (1-7/8 in.) and was placed symmetrically within the section grouped in the corners with a center-to-center spacing between the bars of 2.5 times the diameter of the bars. Altogether, five steel shapes with three concrete strengths means 15 total sections were selected each for RCFT and CCFT, and four steel shapes with three reinforcing configurations and three concrete strengths means 36 total sections were selected each for strong and weak axis bending of SRC.

With the selected CFT sections, the full range of permitted steel ratios is examined, including those associated with noncompact and slender sections. However, local buckling is neglected in this study, both by not modeling it in the inelastic analyses and by not including the strength reductions in the design strength calculations. Thus, the results of this study are only strictly applicable to compact sections. Nonetheless, it is expected that the recommendations developed in this study can be extended to noncompact and slender sections when the appropriate local buckling strength reductions are applied. This is consistent with the development of the direct analysis method for steel structures where local buckling was also neglected (Surovek-Maleck and White 2004b).

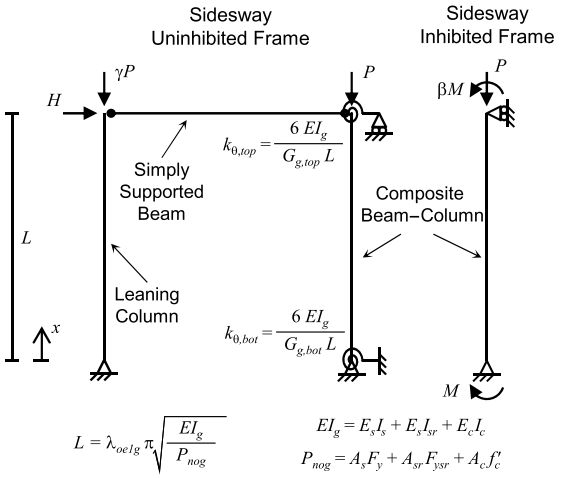

Fig. 1. Schematic of the benchmark frames (reprinted from Denavit et al. 2014, © ASCE)

Frames

A set of small nonredundant frames were described and used in previous stability studies on structural steel members (Kanchanalai 1977; Surovek-Maleck and White 2004b). The set includes both sidesway-inhibited and sidesway-uninhibited frames and a range of slenderness, end constraints, and leaning column loads. The set of frames was expanded and the frame parameters were generalized for use with composite sections in this study. The frames are shown schematically in Fig. 1. The sidesway-uninhibited frame is described by a slenderness value (λ_{oe1g}), which defines the length of the column, a pair of end restraint parameters ($G_{g,\text{top}}$ and $G_{g,\text{bot}}$), which define the stiffness of the rotational spring at the top and bottom of the column, and the leaning column load ratio (γ), which defines the amount of load allocated to the leaning column. The sidesway-inhibited frame is defined by the same slenderness value (λ_{oe1g}) and the end moment ratio (β), which defines the relative values of moment applied at each end. The values of these parameters selected for the frames are described in Tables 2 and 3; a total of 80 frames were selected. The subscript g in the end restraint parameters and slenderness value denotes that these values are defined with respect to gross section properties.

Second-Order Elastic Analysis of Benchmark Frames

The second-order elastic analysis results described in this paper were obtained from the solution of the governing differential equation [Eq. (1)] using the appropriate boundary conditions (Table 4) and the coordinate system as shown in Fig. 1. Closed-form solutions were obtained for displacement and moment along the length of the column using a computer algebra system. This approach is computationally expeditious and accurate for moderate displacements; however, only flexural deformations are included. Where

Table 2. Benchmark Frame Variations (Reprinted from Denavit et al. 2014, © ASCE)

Frame	Slenderness	End restraint	Leaning column load ratio	End moment ratio	Number of frames
Sidesway-uninhibited	4 values $\lambda_{oe1g} = \{0.22, 0.45, 0.67, 0.90\}$	4 value pairs (Table 3)	4 values $\gamma = \{0,1,2,3\}$	N/A	64 ($= 4 \times 4 \times 4$)
Sidesway-inhibited	4 values $\lambda_{oe1g} = \{0.45, 0.90, 1.35, 1.90\}$	N/A	N/A	4 values $\beta = \{-0.5, 0.0, 0.5, 1.0\}$	16 ($= 4 \times 4$)

Table 3. End Restraint Value Pairs (Reprinted from Denavit et al. 2014, © ASCE)

Pair	$G_{g,\text{top}}$	$G_{g,\text{bot}}$
A	0	0
B	1 or 3[a]	1 or 3[a]
C	0	∞
D	1 or 3[a]	∞

[a]3 when $\gamma = 0$; 1 otherwise.

Table 4. Benchmark Frame Boundary Conditions

Boundary condition	Sidesway-uninhibited	Sidesway-inhibited
1	$v(0) = 0$	$v(0) = 0$
2	$-EI_{\text{elastic}} v''(0) = -k_{\theta,\text{bot}} v'(0)$	$-EI_{\text{elastic}} v''(0) = M$
3	$-EI_{\text{elastic}} v'''(L) - Pv'(L) = H + \frac{\gamma P}{L} v(L)$	$v(L) = 0$
4	$-EI_{\text{elastic}} v''(L) = k_{\theta,\text{top}} v'(L)$	$-EI_{\text{elastic}} v''(L) = \beta M$

necessary, the effective length factor (K) for the benchmark frames was back-calculated from the critical load obtained using the same differential equation and boundary conditions

$$v''''(x) + \frac{P}{EI_{\text{elastic}}} v''(x) = 0 \tag{1}$$

where v = lateral deflection; P = axial compression; and EI_{elastic} = elastic flexural rigidity of the column.

Second-Order Inelastic Analysis of Benchmark Frames

The second-order inelastic analysis results described in this paper were obtained from finite-element analyses. Key aspects of the model are summarized here and a full description is available elsewhere (Denavit and Hajjar 2014). The columns were modeled using a distributed plasticity mixed beam finite-element formulation implemented in the *OpenSees* framework (McKenna et al. 2000). Geometric nonlinearity is captured using a total Lagrangian formulation assuming small strains and moderate rotations in the corotational frame and is coupled with an accurate geometric transformation to the global frame. With multiple elements along the length of the column, large displacement and rotation behavior is captured accurately.

Material nonlinearity is captured using a number of fiber cross sections along the length of each element. The uniaxial constitutive relations assigned to each fiber were selected to correspond to assumptions common in the development of design recommendations (e.g., neglecting steel hardening and concrete tension strength) and are comparable to those used in commensurate studies (Surovek-Maleck and White 2004b). Slip between the steel and concrete elements was neglected. Although slip may be important in understanding the local behavior of composite columns, most connections in moment frames will include some bearing components or through bolts internal to the composite member that will limit slip in the connection region. In addition, Hajjar et al. (1998) have shown that connection slip, where it is allowed, rarely impacts the global response of composite structural systems. As noted previously, local buckling of the steel tube and other steel components was also neglected.

Elastic–perfectly plastic constitutive relations and the Lehigh residual stress pattern (Galambos and Ketter 1959) were used to model the wide-flange steel shapes. Reinforcing steel was also modeled as elastic–perfectly plastic, but assumed to have negligible residual stress. Residual stresses in cold-formed steel tubes vary through thickness. To allow a reasonable fiber discretization of the CFT sections, residual stresses were included in the constitutive relation. A multilinear constitutive relation was used in which the stiffness decreases at 75, 87.5, and 100% of the yield stress to approximate the gradual transition into plasticity observed in cold-formed steel (Abdel-Rahman and Sivakumaran 1997). In addition, the yield stress in the corner region of the rectangular members was increased to account for the additional work hardening in that region.

The Popovics concrete model was selected, with the peak compressive stress taken as f'_c or greater to account for confinement (Denavit and Hajjar 2014). Spalling behavior was incorporated into the model for the cover concrete of SRC sections by overriding the stress-strain response with linear degradation to zero stress starting at two times the strain at peak stress. The modulus of elasticity, E_c, used in the analysis was calculated by Eq. (2) taken from the ACI code (2011) for normal-weight concrete. Eq. (2) is equivalent to the expression in the AISC specification (2010b) when the weight of concrete per unit volume is 2,372 kg/m^3 (148.1 lbs/ft^3). Other expressions for the modulus of elasticity have been proposed as more accurate for high-strength concrete and could have been used in the analysis. However, it is not the intention of this paper to develop design recommendations that implicitly include a correction for any potential inaccuracies in the code specified formula for the concrete modulus; thus the modulus used in the analysis and in the design calculations was chosen to be the same

$$E_c[\text{MPa}] = 4{,}733\sqrt{f'_c[\text{MPa}]} \tag{2}$$

Nominal geometric imperfections equal to the fabrication and erection tolerations in the AISC "Code of Standard Practice for Steel Buildings and Bridges" (AISC 2010a) were modeled explicitly. An out-of-plumbness of $L/500$ was included for the sidesway-uninhibited frames and a half-sine wave out-of-straightness with maximum amplitude of $L/1{,}000$ was included for all frames. The initial out-of-plumbness and initial out-of-straightness were applied in the same direction because this produced the greatest destabilizing effect for these frames.

All frame analyses were performed with six elements along the length of the composite column, each with three integration points. Because the analyses were two-dimensional, strips were used for the fiber section; the nominal height of the strips was 1/30 the section depth (e.g., for a CCFT section, approximately 30 steel and 30 concrete strips of near-equal height were used). The leaning column was modeled with a stiff truss element. The lateral deflections at the

top of the leaning column and composite column were set equal with a numerical constraint. Cross section analysis was performed in lieu of frame analysis for the case of zero applied axial load.

Determination of the limit point was often the objective of the analysis. The limit point was defined as the point in the analysis at which the lowest eigenvalue of the system reached zero or when the maximum longitudinal strain in either tension or compression at any point within any cross section along the length of the member reached 0.05, whichever occurred first. The strain limit was imposed because for some cases such as low or zero applied axial load, the eigenvalue limit may only be reached at very high deformations.

The formulation has been validated against hundreds of experimental results from composite members under a variety of loading conditions and with a wide range of material and geometric properties. These comparisons are presented elsewhere (Denavit and Hajjar 2014) along with more accurate constitutive relations that include behavior (e.g., steel strain hardening and concrete tensile strength) that was neglected for this study.

Evaluation of Current Design Procedures

Flexural Strength

The AISC specification (2010b) allows for the flexural strength of compact composite columns to be computed by the plastic stress distribution method. In this method, the steel components are assumed to have reached a stress of F_y in either tension or compression and the concrete components are assumed to have reached a stress of $0.85f'_c$ in compression (or $0.95f'_c$ for CCFT to account for confinement).

The flexural strength obtained from the inelastic analyses (M_{analysis}) for each section is compared with the nominal strength from AISC (2010b) ($M_{n(\text{AISC 2010})}$) in Fig. 2 (noting that in this study local buckling is neglected). A maximum of 5% unconservative error is desired for beam-column design methodologies (ASCE 1997); this limit is shown in the figure as a dashed line.

For CFT and SRC members in strong-axis bending, the nominal strength from AISC (2010b) is either accurate or conservative. For SRC members in weak-axis bending, the nominal strength from AISC (2010b) is mildly unconservative for some sections, particularly steel dominant sections, overpredicting the strength by up to 8%. The primary cause of error is the deformation compatibility of the steel and concrete, and the fact that the curvature required to activate the plastic stress distribution in the steel section assumed in design is large compared with the curvature at which the concrete reaches its peak moment. The distribution of steel within SRC cross sections makes these differences more pronounced under weak-axis bending. These errors do not occur when the strain compatibility approach defined as an alternative approach in the AISC specification (2010b) and in the ACI code (2011) is used because in these methods the compatibility of the steel and concrete is addressed explicitly. Overall, these unconservative errors are small; however, they will be observed again in subsequent results examining interaction strength.

Axial Strength

In the AISC specification (2010b), the nominal axial compressive strength [P_n, Eq. (3)] is determined from a column curve based on the nominal compressive strength of the column without length effects [P_{no}, Eq. (4) for SRC and Eq. (5) for compact CFT without reinforcement] and the slenderness [λ_{oe}, Eq. (6)]. The slenderness is a function of P_{no}, the effective length (KL), and the effective rigidity [EI_{eff}, Eqs. (7) and (8) for SRC and Eqs. (9) and (10) for CFT]. However, when utilized within the direct analysis method, the axial compressive strength is not necessarily representative of the maximum axial load permitted by the design methodology because required accounting of initial geometric imperfections can impart bending moments that reduce the axial strength. To assess the maximum permitted axial load, a second-order elastic analysis with reduced elastic rigidity and accounting of initial geometric imperfections (e.g., either through the use of notional loads or through direct modeling of the imperfections) must be run to determine the maximum applied downward vertical load that results in required axial compression and bending moment that remain within the strength interaction diagram

$$\frac{P_n}{P_{no}} = \begin{cases} 0.658^{\lambda_{oe}^2} & \text{when } \lambda_{oe} \le 1.5 \\ 0.877/\lambda_{oe}^2 & \text{when } \lambda_{oe} > 1.5 \end{cases} \tag{3}$$

$$P_{no} = F_y A_s + F_{\text{ysr}} A_{sr} + 0.85 f'_c A_c \text{ (SRC)} \tag{4}$$

$$P_{no} = F_y A_s + C_2 f'_c A_c \text{ (CFT)} \tag{5}$$

$$\lambda_{oe} = \frac{KL}{\pi}\sqrt{\frac{P_{no}}{EI_{\text{eff}}}} \tag{6}$$

$$EI_{\text{eff}} = E_s I_s + 0.5 E_s I_{sr} + C_1 E_c I_c \text{ (SRC)} \tag{7}$$

$$C_1 = 0.1 + 2\left(\frac{A_s}{A_c + A_s}\right) \le 0.3 \tag{8}$$

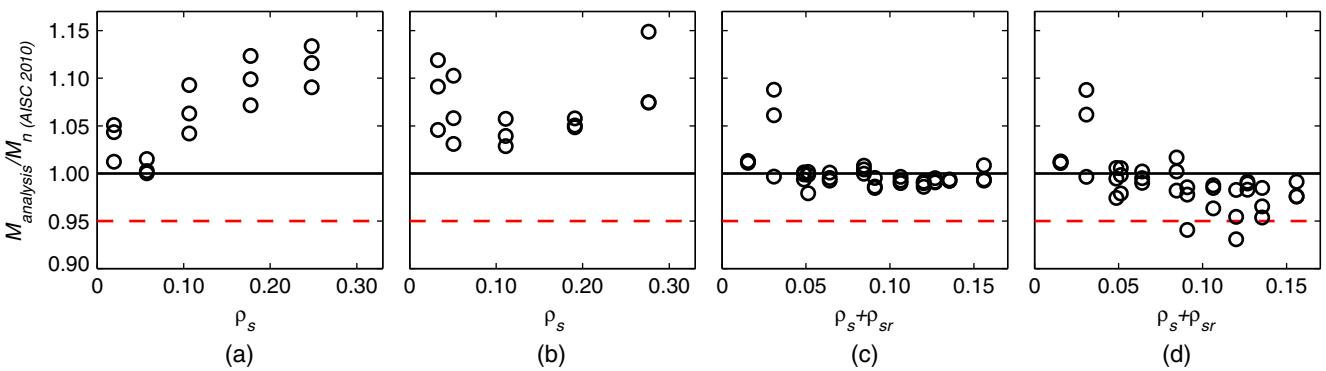

Fig. 2. Flexural strength comparison: (a) CCFT; (b) RCFT; (c) SRC (strong axis); (d) SRC (weak axis)

$$EI_{\text{eff}} = E_s I_s + E_s I_{sr} + C_3 E_c I_c \text{ (CFT)} \tag{9}$$

$$C_3 = 0.6 + 2\left(\frac{A_s}{A_c + A_s}\right) \le 0.9 \tag{10}$$

where A_c = area of concrete; C_2 = 0.85 for RCFT and 0.95 for CCFT; I_s = moment of inertia of the steel section; I_{sr} = moment of inertia of reinforcing bars; I_c = moment of inertia of concrete; and E_s = modulus of elasticity of steel = 200,000 MPa (29,000 ksi).

The commentary of the AISC specification (2010b) recommends the reduced rigidity of composite columns for determining the required strength in the direct analysis method be computed by applying the $0.8\tau_b$ reduction (as for structural steel) to EI_{eff} [Eq. (11)]. The stiffness reduction parameter (τ_b) was developed for structural steel members and depends on the required axial strength (P_r) and the axial yield strength (P_y), a parameter that is undefined for composite members. For the purposes of this study, P_y is taken as P_{no}, resulting in τ_b given by Eq. (12)

$$EI_{\text{DA}} = 0.8\tau_b EI_{\text{eff}} \tag{11}$$

$$\tau_b = \begin{cases} 1.0 & \text{for } P_r/P_{no} \le 0.5 \\ 4(P_r/P_{no})(1 - P_r/P_{no}) & \text{for } P_r/P_{no} > 0.5 \end{cases} \tag{12}$$

In the direct analysis method, initial imperfections must be accounted for either through direct modeling or with representative notional loads. The imperfections were directly modeled in the second-order inelastic analyses (because it is a more exact approach), while they were represented with notional loads in the second-order elastic analyses (because this approach is far more common in design). In each analysis in which the notional load was used, a notional lateral load equal to 0.2% of the vertical load was included. According to Section C2.2b(4) of the AISC specification (2010b), the notional load was taken as a minimum lateral load when the ratio of maximum second-order drift to maximum first-order drift was less than or equal to 1.7 and as an additive lateral load otherwise.

The commentary of the AISC specification (2010b) describes several methods of determining the beam-column interaction strength for composite columns. One method in particular, the plastic stress distribution approach, is used in this study. In this method, a set of points are computed based on the cross-section strength: Point A is the pure axial strength, Point B is the flexural strength, Point C corresponds to a plastic neural axis location that results in the same flexural strength as Point B, and Point D corresponds to the plastic neutral axis location that results in an axial compressive strength one-half of that determined for Point C and represents the maximum moment capacity. The axial component of each of the points is factored down by the ratio P_n/P_{no} to obtain the nominal beam-column strength. The points are further factored down by the resistance factors to obtain the available beam-column strength. These factoring rules and the shape of typical interaction curves can lead to an illogical and potentially unsafe situation in which the factored Point D lies outside the original section strength interaction curve. Because of this, as recommended in the commentary of the AISC specification (2010b), Point D is neglected, resulting in a bilinear interaction diagram defined by Points A, C, and B. This interaction diagram is termed the A-C-B interaction in this paper. More consistent methods of applying stability reductions and resistance factors to avoid the potentially large conservative errors from neglecting Point D are recommended for future research.

An example beam-column interaction diagram is shown in Fig. 3 along with two examples of internal force point traces from elastic analyses as described previously (the lines denoted as Force Trace

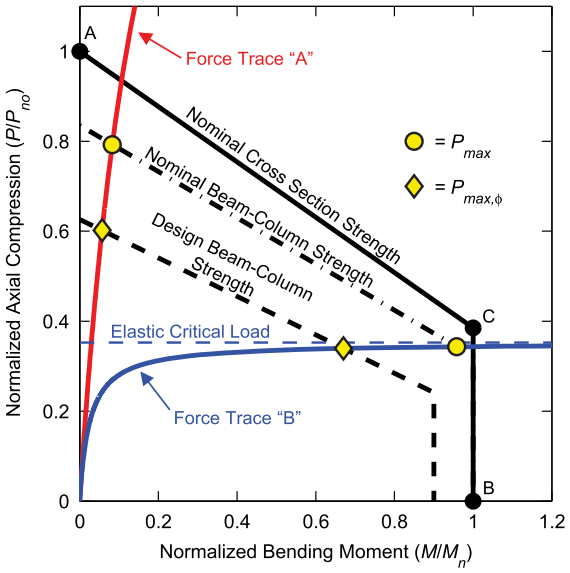

Fig. 3. Example interaction diagram and force trace (adapted from Denavit et al. 2014, © ASCE)

"A" and "B"). The frames (Fig. 1, sidesway-uninhibited) from which the two force traces were derived have the same cross section (RCFT with HSS228.6 × 228.6 × 12.7 and f'_c = 55.2 MPa) and column length ($\lambda_{oe1g} = 0.67$), thus they have the same beam-column strength interaction diagram. The frames differ only in the stiffness of the boundary conditions ($G_{g,\text{top}} = G_{g,\text{bot}} = 0$ for A and $G_{g,\text{top}} = G_{g,\text{bot}} = 1$ for B) and the magnitude of the leaning column load ($\gamma = 0$ for A and $\gamma = 3$ for B). Within the direct analysis method, the effects of boundary conditions and leaning columns are expected to be captured primarily by the second-order elastic analysis in the form of required moment. This is in contrast to the effective length method in which the effective length factor and thus the axial strength plays a more direct role in capturing the effects. One consequence of this difference is the manner in which a particular column appears to fail. The maximum permitted axial load (P_{max}) occurs where the internal force point trace intersects the nominal beam-column strength interaction diagram and the corresponding value including resistance factors ($P_{\text{max},\phi}$) occurs where the internal force point trace intersects the design beam-column strength interaction diagram. As will be shown subsequently, this second value is useful when comparing it with strengths that have also had resistance factors applied. Despite both columns having only vertical load applied, the column with softer boundary conditions and higher leaning column load (B) intersects the interaction diagram with high required moment. Additionally, the difference between P_{max} and $P_{\text{max},\phi}$ is much smaller for B due to the high level of geometric nonlinearity. This would not be the case for either of these observations using the effective length method because the beam-column strength interaction diagram would be reduced significantly for B.

The critical axial load obtained from the second-order inelastic analyses (P_{analysis}) for each section and frame pair is compared with the maximum permitted axial load from the AISC method ($P_{\text{max(AISC 2010)}}$) as a function of slenderness (λ_{oe}) in Fig. 4. In addition to this comparison with nominal strengths, a comparison with available strengths is also presented in Fig. 4. In the comparisons with available strengths, P_{analysis} is multiplied by a resistance factor ($\phi_c = 0.75$) and $P_{\text{max},\phi}$ is used in lieu of P_{max}. The resistance factor for compression is applied to P_{analysis} because only axial

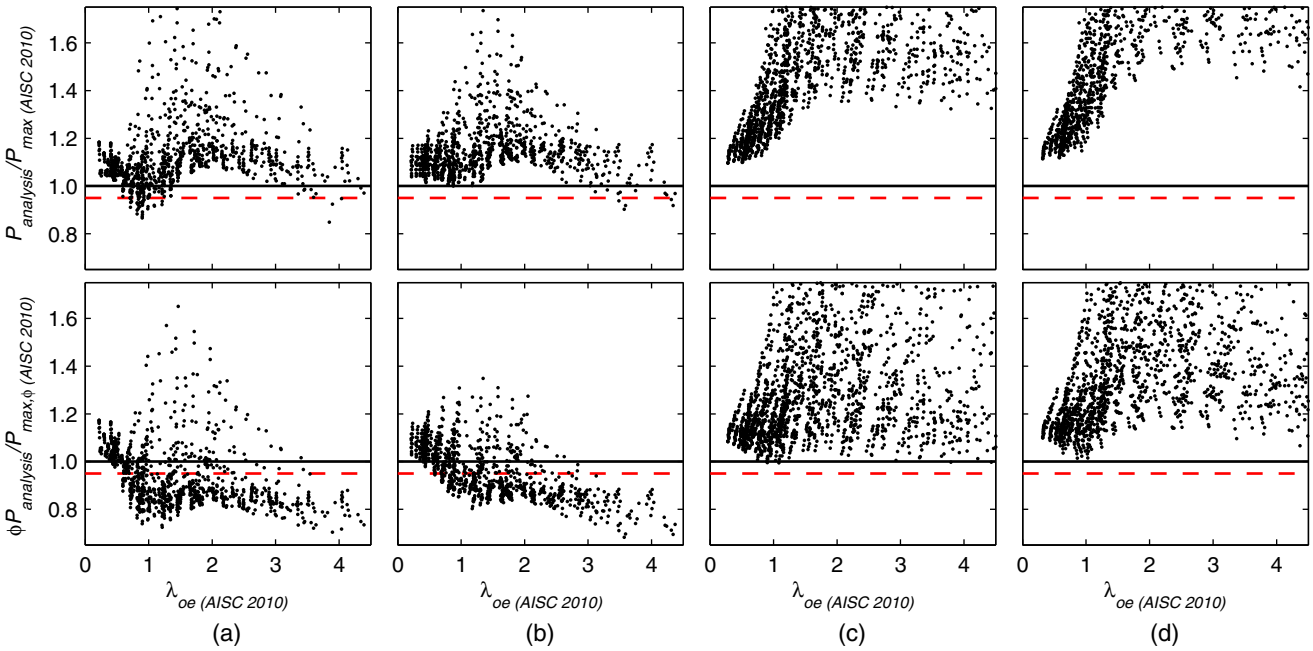

Fig. 4. AISC (2010b) axial strength comparison (reprinted from Denavit et al. 2014, © ASCE): (a) CCFT; (b) RCFT; (c) SRC (strong axis); (d) SRC (weak axis)

loads were applied to the frame in the analysis, with bending moments due only to initial imperfections. From a historical perspective, prior to the requirement for notional loads, the required strength for these cases would not include any moment and the axial load in the column would be compared with the design compression strength ($\phi_c P_n$). Thus, the comparison between $\phi_c P_{\text{analysis}}$ and $P_{\text{max},\phi}$ in Fig. 4 is meant to ensure that the design strength for the sidesway-uninhibited frames is not excessivly liberal when compared with historical approaches or the simply supported columns for which the current resistance factor was originally developed (Leon et al. 2007). Similar comparisons were made in the validaion of the direct analysis method for structural steel (Surovek-Maleck and White 2004b). The dashed line indicates 5% unconservative error.

A wide range of behavior can be seen in the results of Fig. 4. First, within the nominal strength comparison, most cases are shown to be conservative, with the inelastic analysis indicating that the strength is higher than that allowed by the design methodology. The results are generally accurate for the CFT beam columns, with some slight unconservative error for intermediate slenderness CCFTs and for both RCFTs and CCFTs of very high slenderness. For all but the stockiest SRC beam columns, the results are very conservative, indicating a significant underprediction in strength by the design methodology. This is due to the effective stiffness [Eq. (7)] and in particular the C_1 value [Eq. (8)], which are both likely lower than necessary because they were based on the limited range of experimental test data available without the benefit of analyses, such as presented here, which place the experimental results in a broader context.

The strength ratios at the available strength level are lower than those at the nominal strength level. The reason for this can be seen in Fig. 3. While a constant reduction is applied to P_{analysis}, the difference between $P_{\text{max},\phi}$ and P_{max} is not constant, as discussed previously, and for frames in which the geometric nonlinear effects are dominant (such as the case of Force Trace B in Fig. 3), $P_{\text{max},\phi}$ and P_{max} can be similar in value (although the corresponding available axial compression and bending moment strengths are reduced). This fact indicates that the resistance factor applied to the interaction curve is not effective at reducing the maximum permitted applied loads. Stiffness reduction factors are effective for these cases; however, the current stiffness reduction [Eq. (11)] was calibrated for structural steel, which has a higher resistance factor for compression than composite ($\phi_c = 0.9$ versus $\phi_c = 0.75$). To alleviate this error, a stiffness reduction on the order of 0.65 [$\approx 0.877\phi_c$ (Surovek-Maleck and White 2004b)] would be more appropriate.

Interaction Strength

Axial compression-bending moment interaction strength is represented not with single values, but a curve that identifies the strength of the beam-column under combined loading varying from pure bending (typically plotted on the horizontal axis) to pure axial (typically plotted on the vertical axis). To construct this curve, several points on the curve at varying axial loads are determined and straight lines are assumed between the points. The process to determine the individual points is similar to that used to determine the axial strength as described in the previous section. Typical results are presented in Fig. 5 for an example benchmark frame (RCFT with HSS355.6 × 355.6 × 3.2, $f'_c = 27.6$ MPa, sidesway-uninhibited, $\lambda_{oe1g} = 0.67$, $\gamma = 1$, and $G_{g,\text{top}} = G_{g,\text{bot}} = 0$).

The interaction strength according to the second-order inelastic analysis is constructed by selecting a number of axial load values between P_{anaysis} and zero. At each of these values a separate analysis is performed using a nonproportional loading pattern in which the axial compression is applied then held constant, while the lateral load is applied until a limit point is determined. Both the applied loads (Curve 1 in Fig. 5) and internal forces (Curve 2 in Fig. 5) are recorded at the limit point. Only slight differences are noted between limit points obtained from nonproportional analyses and those from proportional analyses. A similar procedure was used to experimentally determine the interaction strength of concrete-filled steel tube beam columns by Perea et al. (2014).

The second-order interaction strength according to the design methodology is determined from design equations. In Fig. 5 the

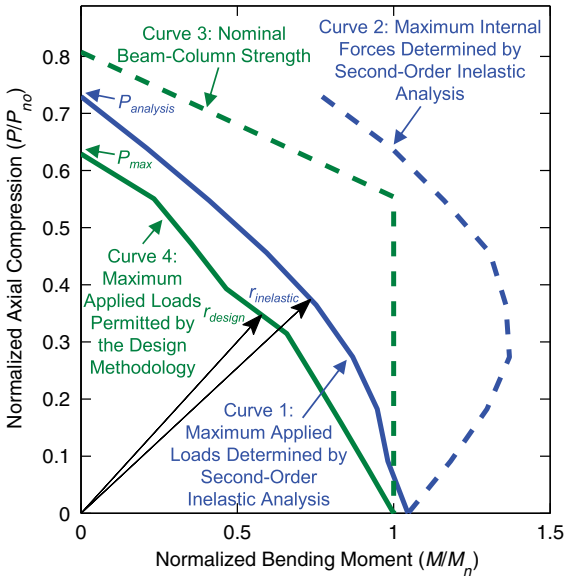

Fig. 5. Comparison of interaction diagram results (adapted from Denavit et al. 2014, © ASCE)

current nominal A-C-B interaction diagram is denoted as Curve 3. Curve 4 in Fig. 5 represents the maximum permitted applied loads using the current design methodology. Under these applied loads, the required axial and flexural strengths determined from a second-order elastic analysis with stiffness reductions and notional loads (where appropriate) lie on the nominal strength interaction diagram.

In Fig. 5, Curve 4 is the envelope of applied loads that are deemed safe by the design methodology. Curve 1 is the envelope of applied loads that are demonstrated to be safe by the inelastic analysis. Thus, regions in which Curve 4 is outside of Curve 1 are considered unconservative.

To quantify error in the design methodology (ε), a radial measure defined by Eq. (13) is selected, where $r_{\text{inelastic}}$ is the distance from the origin to the maximum applied loads determined by second-order inelastic analysis and r_{design} is the distance along the same line to the maximum applied loads permitted by the design methodology. The error varies along the curves, making it necessary to compute its value at many points (i.e., for many angles between the horizontal and vertical axis). Unconservative error by Eq. (13) is represented with negative values

$$\varepsilon = \frac{r_{\text{inelastic}} - r_{\text{design}}}{r_{\text{inelastic}}} \tag{13}$$

The interaction strength comparison results are shown in Figs. 6(a, c, e, and g) for the various section types. For these results the entire suite of benchmark frames has been sorted into a number of bins based on their steel ratio and slenderness [Eq. (6)]. For each of these bins, the maximum unconservative error in the high axial load–low bending moment range, high bending moment–low axial load range, and intermediate range has been determined and displayed. The unconservative errors are shown as positive values in this figure. For example, in Fig. 6(c), for benchmark frames with RCFT cross sections with steel ratio $\rho_s = 0.28$ and slenderness (λ_{oe}) between 2.0 and 3.0, the maximum unconservative error is 0% for cases of high axial load and low bending moment (leftmost number), indicating that no unconservative error was found, 0.5% for cases of high bending moment and low axial load (rightmost number), and 3.5% for intermediate cases (center number). The results of Fig. 6 highlight the worst-case maximum unconservative error, which is useful for the following discussion, but hide the majority of cases, in which no unconservative error is evident. The comparisons of Fig. 6 are performed at the nominal strength level, not including any resistance factors in either the inelastic analysis or elastic design methodology.

The most striking results in Fig. 6 are the large unconservative errors for very slender concrete dominant frames with CFT cross sections [lower right corner of Figs. 6(a and c)]. These errors can be attributed to changes in shape of the strength interaction curve that are not taken into account in the design equations. Interaction strength curves of composite cross sections and short composite beam column are quite convex, particularly for concrete-dominant members. With increases in length, the interaction strength curves become much less convex and often concave. This change is caused by reductions in the flexural rigidity that occur due to material nonlinearity (primarily concrete cracking but also concrete crushing and steel yielding) that occur prior to obtaining the peak strength. The effect is greater for more slender columns because the second-order effects are greater, but also because the ratio of bending moment to axial load is greater, a condition that leads to greater reductions in effective stiffness. This behavior has also been observed experimentally (Perea et al. 2014). The slenderness used to categorize results in Fig. 6 is based on the effective length (KL), so high slenderness can either be caused by long unsupported lengths (L) or by high effective length factors (K) from either soft boundary conditions or high leaning column load. The larger errors are not observed for the SRC columns due to comparatively low EI_{eff} values, indicating that reducing the flexural rigidity in the elastic analysis would be an effective way to reduce these errors.

Other unconservative errors seen in Figs. 6(a and c) are smaller and are typically from either the unconservative error in the axial strength of intermediate slenderness steel-dominant CCFT columns as seen previously or sidesway-inhibited single-curvature cases. The latter cases are challenging due to the fact that cracking and the accompanying stiffness reduction will occur along the entire length of the column as opposed to just the member ends. Again, little unconservative error is noted for SRC columns [Figs. 6(e and g)], with the exception of the moment strength of steel-dominant SRC columns bent about the weak axis, as discussed previously.

Proposed Changes to the AISC Specification

To address the most salient unconservative errors identified in the previous section, two changes are proposed to the AISC specification. The first change is to adopt the stiffness reduction recommended in the commentary to the AISC specification [Eq. (11)], but define the parameter τ_b to equal 0.8 in all cases for composite columns [Eq. (14)]. The value 0.8 was selected in part because it results in a total stiffness reduction approximately equal to $0.877\phi_c$, just as with the reduction for structural steel (Surovek-Maleck and White 2004a)

$$\tau_b = 0.8 \tag{14}$$

The second change is to modify the formulas for EI_{eff} for both SRC and CFT columns [Eqs. (15)–(18)]. This change eliminates the 0.5 factor on the contribution from the steel reinforcing and alters the concrete contribution factors C_1 and C_3. Analyses have shown a constant concrete contribution factor (i.e., $C_1 = 0.7$ and $C_3 = 0.9$) can accurately capture axial strength (Denavit and Hajjar 2014). However, the poorer behavior of more concrete dominant columns under axial compression and bending moment justifies

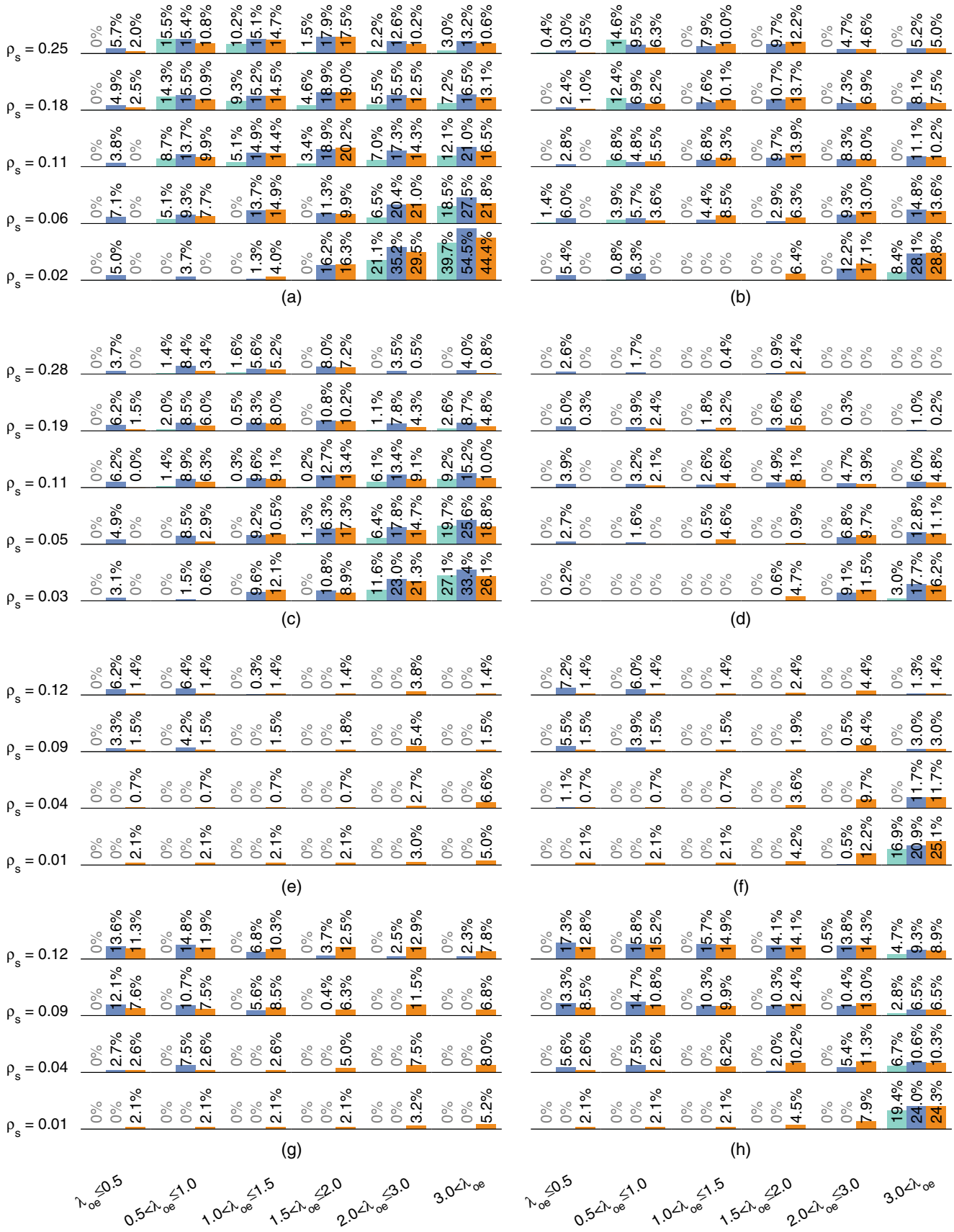

Fig. 6. Maximum unconservative error of interaction strength: (a) CCFT, AISC (2010b); (b) CCFT, proposed; (c) RCFT, AISC (2010b); (d) RCFT, proposed; (e) SRC (strong axis), AISC (2010b); (f) SRC (strong axis), proposed; (g) SRC (weak axis), AISC (2010b); (h) SRC (weak axis), proposed

the further reduction for these sections. The specific values in C_1 and C_3 were selected to obtain good results with little unconservative error in the following comparison. The proposed formulas represent a significant increase in the EI_{eff} for SRC columns and a slight decrease in the EI_{eff} for some CFT columns. Also, the steel ratio variable in C_1 and C_3 has been modified such that the total steel area (including both the steel shape and the reinforcing) is in the numerator and the gross composite area is in the denominator

$$EI_{\text{eff}} = E_s I_s + E_s I_{sr} + C_1 E_c I_c \text{ (SRC)} \tag{15}$$

$$C_1 = 0.25 + 3\left(\frac{A_s + A_{sr}}{A_g}\right) \leq 0.7 \tag{16}$$

$$EI_{\text{eff}} = E_s I_s + E_s I_{sr} + C_3 E_c I_c \text{ (CFT)} \tag{17}$$

$$C_3 = 0.45 + 3\left(\frac{A_s + A_{sr}}{A_g}\right) \leq 0.9 \tag{18}$$

Axial Strength

The proposed changes do not alter the flexural strength, so axial strength will be examined first. Axial strength comparison results are shown in Fig. 7, which was constructed in the same manner as Fig. 4 but using the two proposed changes in the design methodology. These results show that the proposed changes are effective at both reducing the discrepancy between CFT and SRC columns and reducing the unconservative error seen in the available strength comparison for high slenderness CFT columns. The error for intermediate slenderness steel-dominant CCFT columns remains because the proposed changes were not specifically designed to address that error. The proposed changes introduce some unconservative error to high slenderness SRC columns for the available strength comparison (i.e., with reduction factors applied); this is an unfortunate consequence of reducing the overall error in the methodology, however, cases of such high slenderness are rare in practice.

The key difference between CFT and SRC columns that necessitates the difference in EI_{eff} [i.e., Eq. (15) versus Eq. (17)] is the distribution of steel within the composite cross sections. In SRC columns, the steel is typically more centrally located and there exists cover concrete. The selected sections are representative of a wide variety of typical columns, but all have cover equal to the minimum allowed (ACI 2011). If cover in excess of the minimum be used, the strength of the column may decrease and a smaller value of C_1 may be appropriate.

Interaction Strength

Interaction strength comparison results are shown in Figs. 6(b, d, f, and h) for the various section types. The proposed changes are effective at reducing the maximum unconservative errors for CFT. Similar to the axial strength results, the proposed changes introduce greater maximum unconservative errors for the SRC columns in some of the ranges of steel ratio and slenderness. The error in the weak axis flexural strength of steel-dominant SRC columns remains. The largest unconservative errors for all section types occur with the most slender frames, specifically those frames where $P_{\max}/P_{no} < 0.15$, in other words, under gravity-only loading, the columns in these frames can support less than 15% of their squash load. This ratio can be used by engineers to identify stability-sensitive structures. When the maximum permitted axial loads are this low, it would be advisable to use further stiffness reductions to avoid excessive unconservative error. One option is to use $\tau_b = 0.4$ in place of Eq. (14). Another option is to calculate the stiffness for the composite member as though it were bare steel. Both of these options were found to reduce the unconservative error to acceptable levels or eliminate it altogether. However, care should be taken when selecting an elastic stiffness that differs significantly from the expected stiffness because unrealistic distributions of moment in the beams and columns can arise.

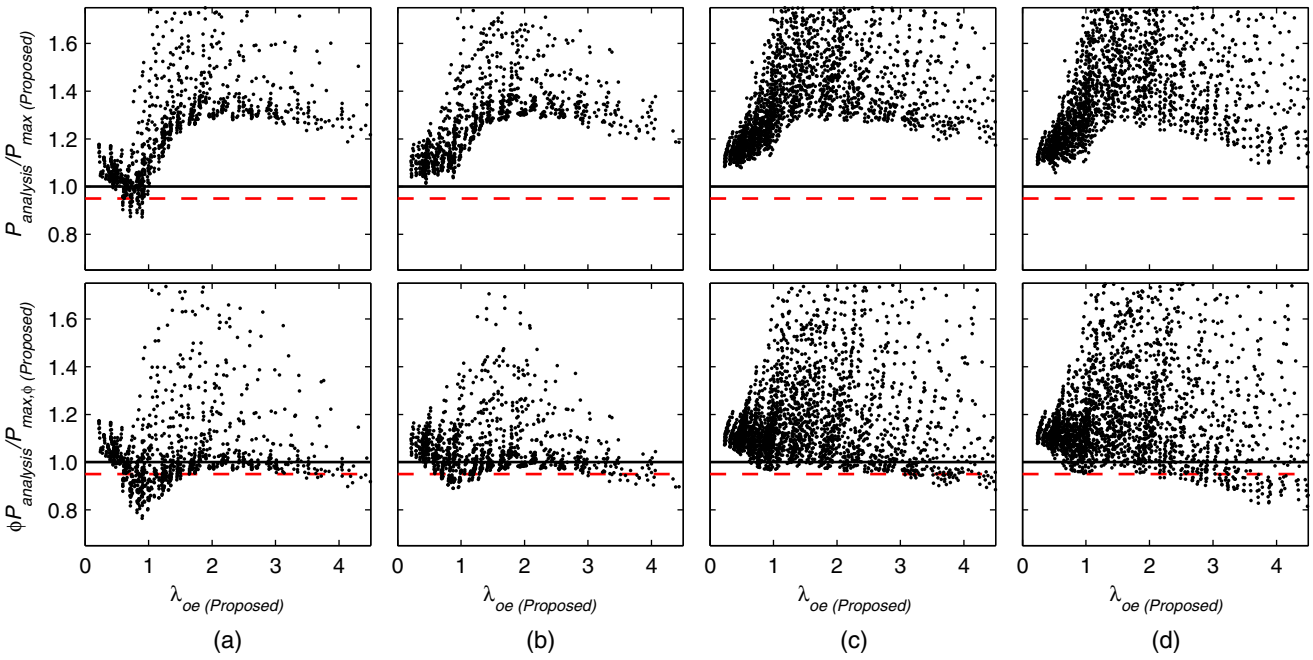

Fig. 7. Proposed axial strength comparison: (a) CCFT; (b) RCFT; (c) SRC (strong axis); (d) SRC (weak axis)

Alternative Stiffness Reduction

Due to the cumbersome nature of a stiffness reduction that varies with axial load, provisions in the AISC specification (AISC 2010b) allow the engineer to use $\tau_b = 1.0$ if an additional 0.1% of the gravity load is applied as a notional load. The proposed τ_b for composite columns [Eq. (14)], however, does not vary with load, making such a substitution both less necessary and less accurate. The additional notional load required to reduce the strength by an amount equivalent to the effect of using $\tau_b = 0.8$ is on the order of 1% for cases in which elastic buckling controls. Such high additional notional loads would be overly conservative in other frames. It is recommended that the use of $\tau_b = 1.0$ in exchange for a higher notional load not be permitted for composite columns. For the case of a structure containing both composite columns and highly loaded ($P_r > 0.5P_y$) steel columns, a conservative approach to avoid a variable stiffness would be to apply the additional notional load so that $\tau_b = 1.0$ can be used for the steel columns and maintain $\tau_b = 0.8$ for the composite columns.

Effective Length Method

The effective length method was the primary method of design in the AISC specification (AISC 2010b) prior to the direct analysis method, and is still allowed as an option to the engineer for cases in which the ratio of maximum second-order drift to maximum first-order drift is less than or equal to 1.5. The effective length method differs from the direct analysis method in that no stiffness reduction is used, notional loads are minimum lateral loads for all cases (because the effective length method is limited to cases in which the ratio of maximum second-order drift to maximum first-order drift is less than 1.5), and the compressive strength is based on the effective length, KL. The use of this method was studied in a similar fashion to what has been shown here for the direct analysis method. The proposed EI_{eff} [Eqs. (15)–(18)] was used for the elastic stiffness in the second-order elastic analysis, and the K factor was determined from the governing differential equation [Eq. (1)] as noted previously. Minimal unconservative error was found within the axial strength results, however, the maximum unconservative error in the intermediate and high moment ranges was found to be greater than for the direct analysis method, particularly for the high slenderness cases. Interaction strength comparison results for SRC columns bent about the weak axis are presented in Fig. 8. The data in Fig. 8 are presented in the same manner as in Fig. 6, with the exception that cases in which the ratio of maximum second-order drift to maximum first-order drift is greater than 1.5 are excluded. Had these cases not been excluded, the maximum errors would be greater. Other section types showed similar trends in the results.

These increased errors can be attributed to the change in shape of the interaction strength as the column slenderness increases. Without stiffness reductions to account for the inelasticity (e.g., concrete cracking and partial steel yielding) that occurs prior to the ultimate load being reached under axial compression plus bending moment, an interaction strength diagram based on section strength is too convex. To alleviate this error, it is recommended that when using the effective length method, the interaction diagram should be taken as described in Section H1.1 of the AISC specification (AISC 2010b) instead of the A-C-B interaction diagram described and used previously. As seen in Fig. 8, using the interaction diagram from Section H1.1, the maximum unconservative errors are approximately equal to those for the direct analysis method. Alternatively, in lieu of using the interaction diagram from Section H1.1, the elastic stiffness could be taken as a value less than EI_{eff}, although an appropriate value would need to be calibrated.

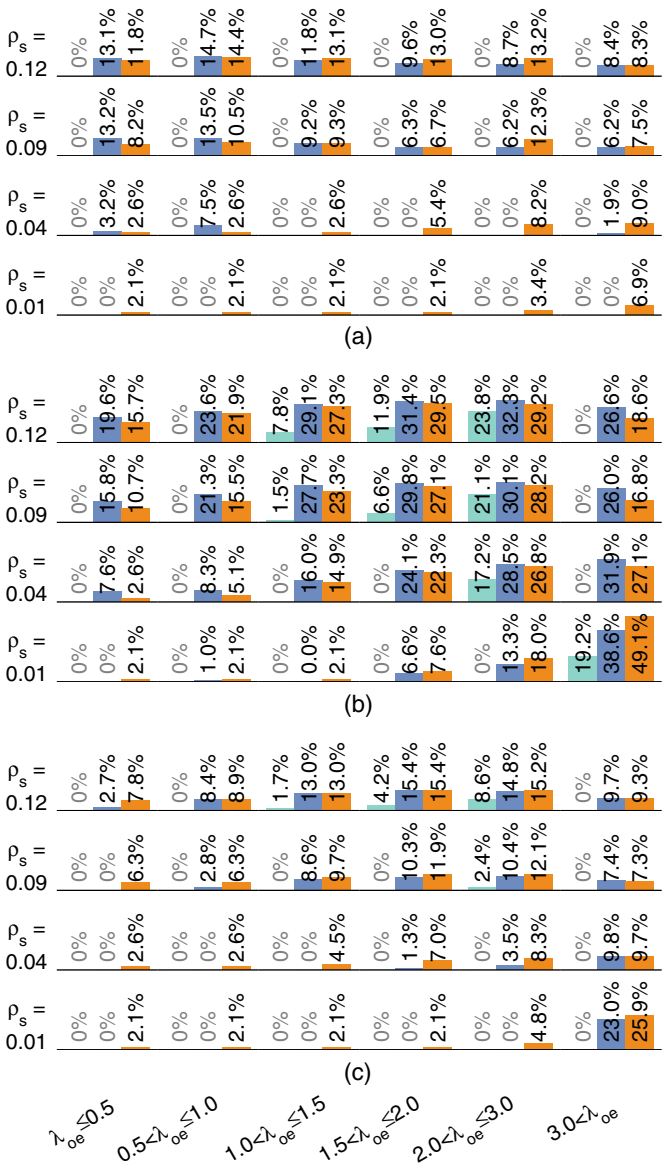

Fig. 8. Maximum unconservative error of interaction strength for the effective length method: (a) SRC (weak axis), AISC (2010b), A-C-B interaction; (b) SRC (weak axis), proposed, A-C-B interaction; (c) SRC (weak axis), proposed, Section H1.1 interaction

Illustrative Example

With the aim of broad applicability, this study has focused on abstract frames and results have been presented in normalized terms. To aid in the understanding of the results, this section presents practical examples. The column cross section for all the examples are the same, a rectangular CFT column constructed of an HSS203.2 × 203.2 × 9.5 (HSS8 × 8 × 3/8) of typical strength [$F_y = 317$ MPa (46 ksi)] and filled with normal-strength concrete [$f'_c = 34.5$ MPa (5 ksi)]. The steel ratio of this section is 16.3%, an intermediate value for CFT members. The effective stiffness is $EI_{\text{eff}} = 10{,}786\ \text{kN} \cdot \text{m}^2 (3.76 \times 10^6\ \text{kip} \cdot \text{in.}^2)$ according to Eq. (17) and the nominal section compressive strength is $P_{no} = 3{,}127$ kN (703 kips). If this member was used as a leaning column or a column in a braced frame ($K = 1$) with a floor height of 4.27 m (14 ft), then the slenderness would be $\lambda_{oe} = 0.731$ [Eq. (6)]. While not stocky, this slenderness is far from the range in which the highest unconservative errors were determined (e.g., $\lambda_{oe} > 2.5$ as seen in

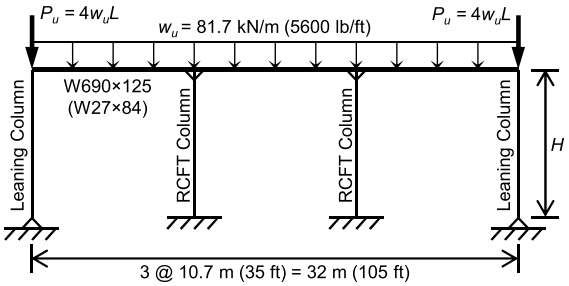

Fig. 9. Multibay industrial frame

Fig. 6). To achieve a very high slenderness, $\lambda_{oe} = 2.5$, the effective length of the column would need to be $KL = 14.59$ m (47.85 ft). At this effective length the slenderness reduction is $P_n/P_{no} = 0.14$ according to the column curve in the AISC specification (AISC 2010b) [Eq. (3)]. This is an impractical height if $K = 1$; however, with leaning column loads the effective length could be achieved with much smaller unbraced lengths. For example, consider a cantilever column with a perfectly rigid connection, two leaning columns, and all three columns supporting the same axial load. For this case, $K = 3.25$ determined using the solution of the governing differential equation [Eq. (1)] as was typically done to determine K in this paper. Thus, $\lambda_{oe} = 2.5$ is achieved when the column height is 4.49 m (14.7 ft). At this length the maximum permitted applied load under a gravity-only load case is $P_{\max} = 305.6$ kN (68.7 kips), resulting in the ratio $P_{\max}/P_{no} = 0.098$, below the 0.15 recommended limit at which unconservative errors may be significant. As an alternative example, consider a variation of the 11-bay industrial frame (Fig. 9) previously analyzed by others (Surovek-Maleck and White 2004a; Deierlein 2003; Martinez-Garcia 2002), where $\lambda_{oe} = 2.5$ is achieved when $H = 5.59$ m (18.4 ft). The effective length for this case was determined as $K = 2.61$ using the story buckling approach described in the commentary of the AISC specification (AISC 2010b) (the differential equation approach used elsewhere in this paper is not applicable to this case). At this length the maximum permitted applied load under a gravity-only load case is $P_{\max} = 441.4$ kN (99.2 kips), resulting in the ratio $P_{\max}/P_{no} = 0.141$, again below the 0.15 recommended limit at which unconservative errors may be significant. While these are not typical cases, they are feasible. It is recommended that should a case such as this arise, further stiffness reductions should be applied as discussed previously.

Further Work

A number of aspects were not addressed in this study and further work on these will be necessary to bring the level of comprehensiveness of the design provisions for steel-concrete composite members to that of either structural steel or reinforced concrete. First, the proposed changes described in this paper have been calibrated to the results of a second-order inelastic analysis model that was validated against experimental results. Validation directly of experiments would increase confidence in the proposals. Additionally, a reliability study is necessary to verify that the current resistance factors are adequate for the new proposals.

The use of the A-C-B interaction diagram, which neglects the balance point, is recommended in the commentary of the AISC specification (AISC 2010b) because of inconsistencies that can arise when applying a stability reduction and resistance factors. However, the A-C-B interaction diagram is very conservative in certain cases. More consistent methods for applying the reductions that would allow the inclusion of the balance point would be beneficial, especially for short concrete dominant columns. Inclusion of the balance point in the interaction diagram would require a reevaluation of the stiffness reduction and potential reduction of EI_{DA}.

The contribution of creep and shrinkage to structural instability was not addressed in this study. The ACI code (ACI 2011) combines and addresses these effects with the use of beta factors when determining the elastic flexural rigidities. A detailed study is warranted to examine how long-term effects on composite columns can be addressed within the AISC specification (AISC 2010b).

Only flexural deformations were considered in the elastic analyses performed in this study, thus only the flexural rigidity (EI) was directly addressed. However, in the general case other rigidities contribute to the stability of the structure and their values should be carefully selected.

In this study, an expression for the elastic flexural rigidity was validated for use in the execution of strength checks. However, this is only one use for EI in the design process. Expressions for EI for other uses, including drift checks and determination of natural frequencies and mode shapes, need to be thoroughly validated.

Conclusions

This paper presents the results of a large parametric study undertaken to assess the in-plane stability behavior of steel-concrete composite columns, evaluate current second-order elastic design provisions within the AISC specification, and propose changes to those provisions where necessary and justified. Comparisons were made between second-order inelastic analysis results, deemed sufficiently accurate to form the basis of design recommendations, and second-order elastic analysis results, representative of the analyses an engineer performs as part of the methodology.

In general, the design methodology was found to be safe and accurate for the majority of cases. However, some unconservative errors were identified, particularly for concrete-dominant members with high slenderness effects. Some significant conservative errors were also identified in which the effective flexural rigidity of SRC members was underestimated in the design provisions.

New effective flexural rigidities for calculating the axial compressive strength and new direct analysis stiffness reductions were proposed to eliminate the most salient unconservative and conservative errors observed in the current design provisions. The proposed beam-column design methodology is safe and accurate for the vast majority of cases of composite member behavior, although further research is recommended to continue to investigate the axial compressive strength of steel-dominant intermediate slenderness CCFTs, the weak-axis flexural strength of steel-dominant SRCs, and the long-term behavior of composite columns.

Acknowledgments

The authors are grateful for the advice received from AISC Committee on Specifications Task Committee 5 on Composite Construction and Task Committee 10 on Stability, as well as Professors Donald White, Ronald Ziemian, Gregory Deierlein, and Andrea Surovek regarding this work. This material is based on work supported by the National Science Foundation under Grant Nos. CMMI-0530756 and CMMI-0619047 as part of the George E. Brown, Jr. Network for Earthquake Engineering Simulation (NEES), the American Institute of Steel Construction, Georgia Institute of Technology, University of Illinois at Urbana-Champaign, and Northeastern University.

References

Abdel-Rahman, N., and Sivakumaran, K. S. (1997). "Material properties models for analysis of cold-formed steel members." *J. Struct. Eng.*, 10.1061/(ASCE)0733-9445(1997)123:9(1135), 1135–1143.

ACI (American Concrete Institute). (2011). "Building code requirements for structural concrete and commentary." Farmington Hills, MI.

AISC. (2010a). "Code of standard practice for steel buildings and bridges." Chicago.

AISC. (2010b). "Specification for structural steel buildings." Chicago.

ASCE. (1997). "Effective length and notional load approaches for assessing frame stability: Implications for American steel design." Reston, VA.

Deierlein, G. G. (2003). "Background and illustrative examples of proposed direct analysis method for stability design of moment frames." *Rep. to Task Committee 10*, AISC, Chicago.

Denavit, M. D., and Hajjar, J. F. (2014). "Characterization of behavior of steel-concrete composite members and frames with applications for design." *Newmark Structural Laboratory Rep. Series, Newmark Structural Laboratory Rep. NSEL-034*, Univ. of Illinois at Urbana-Champaign, Urbana, IL.

Denavit, M. D., Hajjar, J. F., Leon, R. T., and Perea, T. (2014). "Analysis and design of steel-concrete composite frame systems." *Structures Congress 2014*, ASCE, Reston, VA, 2605–2616.

Galambos, T. V., and Ketter, R. L. (1959). "Columns under combined bending and thrust." *J. Eng. Mech. Div.*, 85(2), 1–30.

Hage, S. E., and MacGregor, J. G. (1974). "The second-order analysis of reinforced concrete frames." *Structural Engineering Rep. No. 49*, Dept. of Civil Engineering, Univ. of Alberta, Edmonton, AB, Canada.

Hajjar, J. F., Schiller, P. H., and Molodan, A. (1998). "A distributed plasticity model for concrete-filled steel tube beam-columns with interlayer slip." *Eng. Struct.*, 20(8), 663–676.

Kanchanalai, T. (1977). "The design and behavior of beam-columns in unbraced steel frames." *CESRL Rep. No. 77-2*, Structures Research Laboratory, Dept. of Civil Engineering, Univ. of Texas at Austin, Austin, TX.

Leon, R. T., Kim, D. K., and Hajjar, J. F. (2007). "Limit state response of composite columns and beam-columns. Part 1: Formulation of design provisions for the 2005 AISC specification." *Eng. J.*, 44(4), 341–358.

Martinez-Garcia, J. M. (2002). "Benchmark studies to evaluate new provisions for frame stability using second-order analysis." M.S. thesis, Dept. of Civil and Environmental Engineering, Bucknell Univ., Lewisburg, PA.

McKenna, F., Fenves, G. L., and Scott, M. H. (2000). "Open system for earthquake engineering simulation." Univ. of California, Berkeley, CA, ⟨http://opensees.berkeley.edu⟩.

Perea, T., Leon, R. T., Hajjar, J. F., and Denavit, M. D. (2014). "Full-scale tests of slender concrete-filled tubes: Interaction behavior." *J. Struct. Eng.*, 10.1061/(ASCE)ST.1943-541X.0000949, 04014054.

Surovek-Maleck, A. E., and White, D. W. (2004a). "Alternative approaches for elastic analysis and design of steel frames. I: Overview." *J. Struct. Eng.*, 10.1061/(ASCE)0733-9445(2004)130:8(1186), 1186–1196.

Surovek-Maleck, A. E., and White, D. W. (2004b). "Alternative approaches for elastic analysis and design of steel frames. II: Verification studies." *J. Struct. Eng.*, 10.1061/(ASCE)0733-9445(2004)130:8(1197), 1197–1205.